Available online at www.sciencedirect.com
ScienceDirect
Ceramics International 34 (2008) 859–862
CERAMICS INTERNATIONAL
www.elsevier.com/locate/ceramint

X-ray absorption study on $LiNi_{0.8}Co_{0.15}Al_{0.05}O_2$ cathode material for lithium-ion batteries

Takamasa Nonaka [a,*], Chikaaki Okuda [a], Yoshiki Seno [a], Kunihito Koumoto [b], Yoshio Ukyo [a]

[a] *Toyota Central R&D Labs., Inc., Nagakute, Aichi 480-1192, Japan*
[b] *Nagoya University, Graduate School of Engineering, Aichi 464-8603, Japan*

Available online 29 September 2007

Abstract

$LiNi_{0.8}Co_{0.15}Al_{0.05}O_2$, being one of the promising cathode materials for lithium-ion batteries, shows distinct capacity fades after charge/discharge cycling and/or storage at high temperatures. The origin of the capacity fade has been explored by investigating the electronic and structural changes of the cathode material using X-ray absorption spectroscopy (XAS). Ni K-edge XAS measurements were performed in two different modes: surface-sensitive conversion electron yield (CEY) mode and bulk-sensitive transmission mode. Ni K-edge XANES data revealed that, after the cycling and aging tests, the bulk-averaged Ni valences were reduced, implying the existence of divalent Ni atoms. Further reductions of Ni atoms were observed at the surface of the cathode material particles, and the ranges of the Ni valence change upon charging became narrower, indicating the existence of the Ni atoms that did not oxidize. These changes which occur prominently at the surface are probably the main causes of the capacity fade.

Keywords: B. Spectroscopy; B. X-ray methods; D. Transition metal oxides; E. Batteries

1. Introduction

$LiNi_{0.8}Co_{0.15}Al_{0.05}O_2$ is being considered as a promising cathode material because of its improved stability and electrochemical performance brought by Co and Al substitutions for Ni in $LiNiO_2$ [1]. $LiNi_{0.8}Co_{0.15}Al_{0.05}O_2$ remains as a single rhombohedral phase during charge/discharge cycling, allowing a high cycling reversibility. In spite of such improvements, $LiNi_{0.8}Co_{0.15}Al_{0.05}O_2$ still has the problem of deteriorations such as capacity fading and the increase in impedance [2]. These deteriorations occur during use (i.e. on electrochemical cycling) and/or on storage at high temperatures, being one of the most crucial problems which should be overcome for applications requiring a very long life, such as electric vehicles. Although the mechanism of deteriorations is considered to be quite complicated, it was found that, in the case of the battery using $LiNi_{0.8}Co_{0.15}Al_{0.05}O_2$, the increase in impedance is predominantly attributed to the cathode [2]. It has been also reported that, in the battery using $LiNi_{0.8}Co_{0.2}O_2$, the charge-transfer resistance at the cathode–electrolyte interface is the main cause of the impedance increase [3].

In this study, conversion electron yield (CEY) XAFS [4] at Ni K-edge was employed as a tool to explore the near-surface regions of the cathode particles. Furthermore, near-surface-averaged information was compared with bulk-averaged information on cathode material particles using both CEY-XAFS and conventional XAFS in the transmission mode. This combined probe has a potential to offer a new insight into the battery deterioration mechanism. The purposes of this study are (1) to clarify the changes in the oxidation state and local structure of Ni during charge/discharge for a fresh (not deteriorated) battery, and (2) to elucidate the changes induced by cycle and aging tests.

2. Experimental procedure

The cathode sheets removed from 18650-type cells were used as samples [2]. The cell consisted of a cathode sheet, an anode sheet, an electrolyte and a separator. The cathode sheet was a thin Al foil on both sides of which ~20 μm thick

* Corresponding author. Tel.: +81 561 63 6126; fax: +81 561 63 6448.
E-mail address: nonaka@mosk.tytlabs.co.jp (T. Nonaka).

0272-8842/$34.00
doi:10.1016/j.ceramint.2007.09.036

electrode mixtures were coated, containing 85 wt% $LiNi_{0.8}Co_{0.15}Al_{0.05}O_2$, 10 wt% conductive materials and 5 wt% polyvinylidene fluoride (PVDF) binder. The $LiNi_{0.8}Co_{0.15}Al_{0.05}O_2$ cathode material comprised of 10–15 μm secondary particles, each of which was composed of smaller primary particles. The cells which exhibited various levels of capacity fading were prepared: fresh cells, cycle tested cells (1000 cycles at 60 °C) and aging tested cells (storage at 60 °C for a year). The discharge capacity of each cell condition is 160, 123 and 125 mAh/g, respectively. In order to investigate the change accompanied by charging (Li-deintercalation), the cells with various states of charge were prepared for each cell condition. The Li contents in $Li_{1-x}Ni_{0.8}Co_{0.15}Al_{0.05}O_2$ ($0.07 < x < 0.71$) were determined by inductively coupled plasma-atomic emission spectroscopy (ICP-AES).

The CEY and transmission XAFS measurements were performed on the beamline BL16B2 of the SPring-8 (Hyogo, Japan). A newly developed detector was used for the CEY-XAFS. A sample surrounded by an atmospheric pressure helium gas is irradiated with X-rays, which arise the emission of electrons (predominantly Ni KLL Auger electrons in this case) from the sample surface. Each electron induces the cascade ionization of He atoms, generating a bunch of He ions and secondary electrons. The resultant He ions and secondary electrons are collected with high-voltage biased carbon electrodes. Schroeder et al. [5] has reported that the probing depth of Ni K-edge CEY-XAFS for NiO is experimentally estimated to be ∼90 nm. The probing depth of the present measurement was estimated to be almost the same value as theirs since the near-surface region of the $Li_{1-x}Ni_{0.8}Ni_{0.8}Co_{0.15}Al_{0.05}O_2$ particles exhibits Ni–O-like properties as shown later.

3. Results and discussion

Fig. 1 shows representative Ni K-edge XANES spectra of $Li_{1-x}Ni_{0.8}Co_{0.15}Al_{0.05}O_2$ ($x = 0.07$, 0.68) obtained in both the transmission and CEY-XAFS for the fresh cell. It can be seen that, in both edges, the shapes and signal-to-noise ratios of XANES spectra obtained in different techniques are completely identical. This ensures the validity of the quantitative comparison of the results deduced from the two techniques at least in XANES region. As Li is deintercalated (x increases), the entire pattern of the Ni K-edge spectrum shifts to higher energies, indicating the oxidization of Ni atoms.

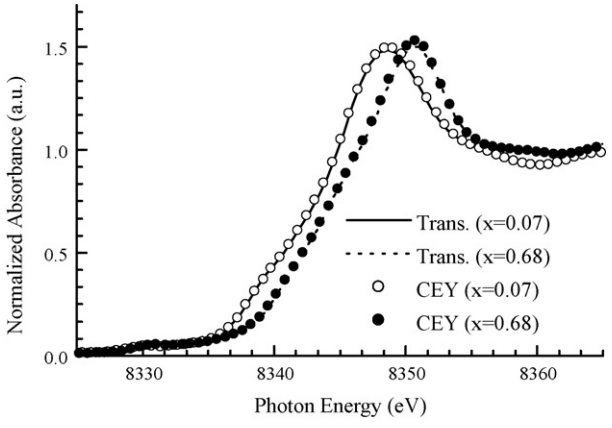

Fig. 1. XANES spectra for $Li_{1-x}Ni_{0.8}Co_{0.15}Al_{0.05}O_2$ at the Ni K-edge obtained in transmission XAFS (Trans.) and conversion electron yield XAFS (CEY).

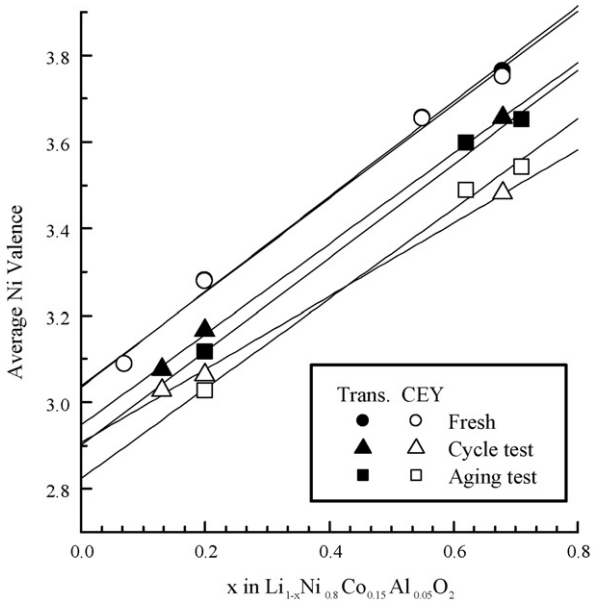

Fig. 2. Comparison of average Ni valences estimated using the edge positions of the XANES spectra along with approximate lines.

The value of the energy at half-step height (where normalized absorbance = 0.5) was used as a measure of oxidation state. Average Ni valences were estimated using the analytical curve proposed by Mansour et al. They have found a quadratic dependence for edge energy (at half-step height) versus Ni valence using NiO, stoichiometric $LiNiO_2$, and $KNiIO_6$ as reference compounds for Ni^{2+}, Ni^{3+} and Ni^{4+}, respectively [6]. Fig. 2 shows a comparison of estimated average Ni valences along with approximate lines obtained using least-squares fits. For the fresh cell, the line of the bulk (transmission XAFS) and that of the surface (CEY-XAFS) are almost identical, and change predominantly from trivalent to tetravalent upon charging. As can be clearly seen, after the cycling and aging tests, the bulk-averaged Ni valences become lower than that in the fresh cell throughout all values of x. Further reductions of Ni atoms are observed at the surface of the tested cells. These results indicate that the content of divalent Ni atoms is increased by the cycling and aging tests, especially at the cathode material surface. In addition to the prominent drops in Ni valence, the slopes of the approximate lines for the surface of the tested cells, especially of the cycled cell, are less than that for the fresh cell. This implies the presence of the Ni atoms, most likely divalent Ni, that no longer contribute to the charge compensation of $Li_{1-x}Ni_{0.8}Co_{0.15}Al_{0.05}O_2$.

Fourier-transforms of the Ni K-edge EXAFS spectra for the fresh cell as a function of x in $Li_{1-x}Ni_{0.8}Co_{0.15}Al_{0.05}O_2$ are shown in Fig. 3 (CEY-XAFS). The first peak at around 1.5 Å corresponds to Ni–O interaction and the second one at around 2.5 Å corresponds to Ni–M (M = Ni, Co) interaction. It can be

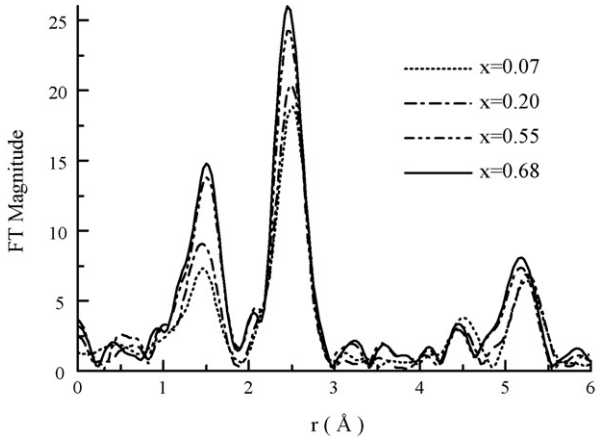

Fig. 3. Fourier-transforms as a function of x for Ni in $Li_{1-x}Ni_{0.8}Co_{0.15}Al_{0.05}O_2$ (fresh cell, CEY-XAFS).

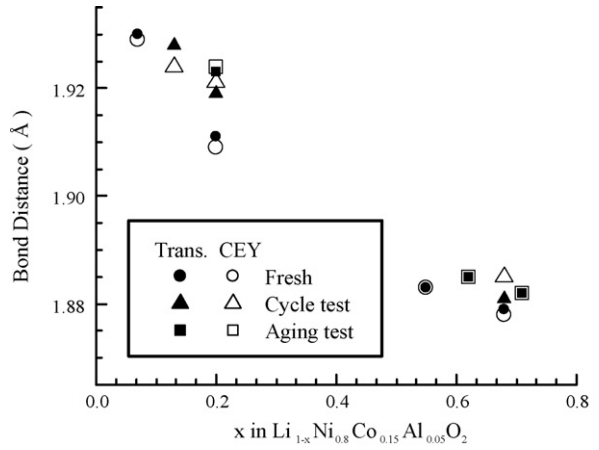

Fig. 4. Variations of the average Ni–O bond lengths obtained by the fitting to the first peak of the Ni K-edge FT.

seen that the amplitude of Ni–O peak increases with charging. The smaller amplitude before charging is well understood by considering the local Jahn–Teller effect of NiO_6 octahedron expected for Ni^{3+} in a low-spin state.

Fig. 4 is the plot of Ni–O bond distances deduced from curve-fits as a function of x in $Li_{1-x}Ni_{0.8}Co_{0.15}Al_{0.05}O_2$. The Ni–O peak, which is actually composed of contributions from four subshells (one Ni^{2+}–O, two Ni^{3+}–Os and one Ni^{4+}–O), was fitted to one Ni–O shell. The bulk- and surface-averaged Ni–O bond distance for the fresh cell decreases with increasing the value of x. This behavior is attributed to the conversion of Ni oxidation state from Ni^{3+} to Ni^{4+}. As described above the Ni^{3+}–O shell is composed of four shorter and two longer bonds, both of which are longer than the Ni^{4+}–O bond [7]. The bulk- and surface-averaged Ni–O bond distances for the cycling and aging tested cells seem slightly longer than those for the fresh cell. This is consistent with the drops in Ni valences observed in XANES spectra. The presence of divalent Ni atoms is expected to result in expanding Ni–O bond distance due to larger Ni^{2+} ionic radius than Ni^{3+} one. Although the certain difference between bulk- and surface-averaged Ni valences is found in the XANES analysis, distinct differences in Ni–O bond distances are not observed within the accuracy limit of the fitting analysis. It should be also noted that all the Ni–O bond distances obtained in this work are much shorter than a distance of 2.08 Å that is expected for pure NiO.

The XANES and EXAFS results are in good agreement with the Abraham et al.'s observation for $LiNi_{0.8}Co_{0.2}O_2$ [8]. Their TEM and electron energy loss spectroscopy (EELS) data showed that the Ni–O like surface layer having NaCl-type structure was existent at the surface of the cathode material particles and it grew during the aging test. They proposed a possible mechanism of the capacity fading; the presence of Ni–O like layer, which may reduce electronic and ionic conductivities, is the main reason for the capacity fading. The similar phenomena are supposed to occur in the case of $LiNi_{0.8}Co_{0.15}Al_{0.05}O_2$.

4. Conclusions

CEY and transmission XAFS techniques were applied to study $LiNi_{0.8}Co_{0.15}Al_{0.05}O_2$ cathode material for Li-ion cells that showed various levels of capacity fading: fresh cell, cycle tested cell and aging tested cell. The conclusions of this study are as follows:

1. Ni K-edge XANES data obtained in the transmission mode showed that the bulk-averaged Ni valence for the fresh cell oxidized from Ni^{3+} to Ni^{4+} upon charging. The bulk-averaged Ni valences for the cycle tested cell and aging tested cell were lower than that for the fresh cell throughout charging.
2. Ni K-edge XANES data obtained in the CEY-XAFS showed that the surface-averaged Ni valence for the fresh cell was lower than the bulk-averaged one. Further reductions of Ni atoms occurred at the surface after the cycle and aging tests and the ranges of Ni valence change upon charging became narrower than that for the fresh cell, indicting the existence of the divalent Ni that did not change upon charging.

Acknowledgements

The authors are grateful to Y. Takeuchi, Y. Itou, O. Hiruta, S. Kawauchi, H. Kondo, K. Dohmae, I. Tajima, H. Nozaki and S. Yamaguchi for their contributions to this work and would like to thank H. Tanida for the development of the software for XAFS measurements.

References

[1] H. Cao, B. Xia, N. Xu, C. Zhang, Structural and electrochemical characteristics of Co and Al co-doped lithium nickelate cathode materials for lithium-ion batteries, J. Alloys Compd. 376 (1–2) (2004) 282–286.
[2] Y. Itou, Y. Ukyo, Performance of $LiNiCoO_2$ materials for advanced lithium-ion batteries, J. Power Sources 146 (1–2) (2005) 39–44.
[3] K. Amine, C.H. Chen, J. Liu, M. Hammond, A. Jansen, D. Dees, I. Bloom, D. Vissers, G. Henriksen, Factors responsible for impedance rise in high power lithium ion batteries, J. Power Sources 97–98 (2001) 684–687.
[4] M. Takahashi, M. Harada, I. Watanabe, T. Uruga, H. Tanida, Y. Yoneda, S. Emura, T. Tanaka, H. Kimura, Y. Kubozono, S. Kikkawa, Eu K-XAFS of

europium dioxymonocyanamide with the conversion He ion yield method, J. Synchrotron Radiat. 6 (1999) 222–224.
[5] S.L.M. Schroeder, G.D. Moggridge, R.M. Ormerod, T. Rayment, R.M. Lambert, What determines the probing depth of electron yield XAS? Surf. Sci. Lett. 324 (1995) L371–L377.
[6] A.N. Mansour, J. McBreen, C.A. Melnedres, An in situ X-ray absorption spectroscopic study of charged $Li_{(1-z)}Ni_{(1+z)}O_2$ cathode material, J. Electrochem. Soc. 146 (8) (1999) 2799–2809.
[7] M. Balasubramanian, X. Sun, X.Q. Yang, J. McBreen, In situ X-ray absorption studies of a high-rate $LiNi_{0.85}Co_{0.15}O_2$ cathode material, J. Electrochem. Soc. 147 (8) (2000) 2903–2909.
[8] D.P. Abraham, R.D. Twesten, M. Balasubramanian, J. Kropf, D. Fischer, J. McBreen, I. Petrov, K. Amine, Microscopy and spectroscopy of lithium nickel oxide-based particles used in high power lithium-ion cells, J. Electrochem. Soc. 150 (11) (2003) 1450–1456.